A STOCHASTIC MODEL FOR EYE MOVEMENTS DURING FIXATION ON A STATIONARY TARGET

R. Vasudevan*
A. V. Phatak
J. D. Smith

Department of Electrical Engineering
University of Southern California
Los Angeles, California 90007

Technical Report No. 71-23

May 1971

Supported by the National Institutes of Health under Grant Nos. GM 16197-03 and RR 0712-04, by the National Science Foundation under Grant No. GK 1834X, and by the National Aeronautics and Space Administration under Grant No. NGL 05-018-022

*On Leave of Absence from the Institute of Mathematical Sciences, Madras, India

ABSTRACT

A stochastic model describing small eye movements occurring during steady fixation on a stationary target is presented. Based on eye movement data for steady gaze, the model has a hierarchical structure; the principal level represents the random motion of the image point within a local area of fixation while the higher level mimics the jump processes involved in transitions from one local area to another. Target image motion within a local area is described by a Langevin-like stochastic differential equation taking into consideration, the microsaccadic jumps pictured as being due to point processes and the high frequency muscle tremor, represented as a white noise. The transform of the probability density function for local area motion is obtained, leading to explicit expressions for their means and moments. Evaluation of these moments based on the model are comparable with experimental results. A physiologically based criterion for the occurrence of local area changes is assumed and the renewal density of these transitions is obtained. These transitions are brought about by the occurrence of large saccades. Hence, our analysis leads us to derive expressions for the mean and moments of the occurrence of large saccades in a given time T. These predictions may be checked against experimental results.

A STOCHASTIC MODEL FOR EYE MOVEMENTS DURING FIXATION ON A STATIONARY TARGET

I. Introduction and Background

System models of human eye movement control in the past have been concerned with eye movements in response to the tracking of moving targets [1,2,3]. Most of these models have involved partitioning of the controller into two subsystems, one for smooth eye movements and another for rapid saccadic changes in eye position. Investigations of eye movement during fixation have not, to the authors' knowledge, been treated in terms of a quantitative model as have eye movements during tracking tasks. The major emphasis of fixation experiments has been to treat the eye movement data as a time series and analyze it via classical statistical methodology. We decided to first examine the more basic phenomenon of eye movements with a steady fixation point as the target. In this mode of operation the eye is not motionless; in fact, a small amount of eye movement [4,5] is apparently necessary for transmission of visual images.

A schematic diagram of the eye during viewing of a stationary target is shown in Fig. 1. The fovea is an anatomically distinct portion of the retina subtending a 2 degree circle of visual field. The eyeball is moved by forces applied via the six extraocular muscles not shown. Our interest here is to study the motion of the retinal image of the target during visual fixation. Based on studies during fixation, eye movements have been classified into three distinct types:

a) microsaccades: these are rapid step-like changes in eye position averaging 6 minutes of arc in amplitude.

b) drift[1]: these low frequency eye movements average 5 minutes of arc in amplitude with rates of 1 minute of arc per second.

c) tremor: this refers to very high frequency oscillations in eye movement ranging from 5-15 seconds of arc in amplitude at frequencies from 30-80 Hz.

---

[1] The physiological term drift indicates all slow eye movements after removal of the microsaccade and tremor components.

The measurement of these small movements during fixation have been reported by several investigators [6,7,8,9,10]. The implications of their work and particularly that of Boyce [11] were indispensible in our formulating a structure for eye movement control during steady gaze.

Experiments designed where the target moves synchronously with eye position thereby maintaining a stabilized image [4,5,12] have demonstrated that small eye movements are necessary for continuous perception of a fixed target. This intriguing evidence of a requirement for movement during fixation leads to the question of how the system generates these movements. Nachmias [7] discusses a relationship between drift and microsaccades; his findings are in accord with those of Cornsweet [10] in proposing that a proportion of the microsaccades are movements that compensate for involuntary drift.

The recent work of Boyce [11] proves to be very significant. His analysis of two dimensional data time series revealed the following characteristics:

a) Recordings of eye position during gaze can be subdivided into a succession of time periods. During each of these short-period fixations, the retinal target image is projected to a discrete portion of the retina, henceforth referred to as a local area.

b) Saccades during gaze at a stationary target have one of two functions: (i) to move the retinal target image suddenly within the local area, or (ii) to move the image to a new local area.

Based on these characteristics, Boyce proposed a qualitative "organizational model" of the system. The successive local areas are presumably contained entirely within the fovea where the highest degree of visual acuity is attained and receptor elements of the retina are most densely packed. In Fig. 2 a representation of target image on the fovea during a period of fixation on a motionless target is shown. The purpose of the next section is to incorporate the above mentioned qualitative properties of eye movements into a quantitative stochastic model of this neurological control system.

II. Eye Movement Model: Formulation of the Structure

The structure of the model proposed here is derived on the basis of the concept of local areas of fixation. It is a quantitative version of the earlier simulation model proposed by Smith and Phatak [13]. The model has a hierarchical configuration with: (1) a principal level that simulates eye movements within a local area of fixation and (2) a higher level that mimics the jump process from one local area to another. The model is developed for application across a one-dimensional visual field in order to keep the analysis tractable and easy to follow. Extension to a two-dimensional visual field can be implemented easily.

A. Model for Local Area

It is apparent that in modeling eye movements within a local area one must consider the drift, tremor and only those microsaccades that occur and stay within the local area. The motion of the target image within a local area of fixation may be modeled very simply by a position control system as shown in Fig. 3.

In Fig. 3, e(t) is the error signal in degrees and $F_0(t)$ is the net force applied to the eyeball in grams. This net force $F_0(t)$ is the sum of three forces: (1) the restoring force ke, due to the position control loop, (2) the tremor force, $F_1(t)$, modeled as a white noise and (3) the saccadic impulsive forces, $F_2(t)$, represented as arising from a stochastic point process. In this representation drift is only the compensatory movement due to the position control loop. It is also assumed here that there is no bias drift caused by the geometry of the experiment and/or anatomical considerations. The reference point θ_{ref} for the position control system is taken as the center of the local area of fixation. The plant is represented as the muscle-eyeball dynamics, which have been modeled in the literature by a number of investigators [14,15,16,17]. An adequate model for our purpose is that due to Robinson [15]. It relates eye position $\theta(t)$ to applied muscle force $F_0(t)$ by a fourth order linear differential equation. The corresponding transfer function is given by

$$(1) \qquad \frac{\theta}{F_0}(s) \triangleq G(s) = \frac{(.667)(1+.214s)}{(1+.3s)(1+.0604s)[1+.00481s+1.03\times 10^{-5}s^2]} \,.$$

The retinal gain k is fixed at unity.

The model in Fig. 3 can be further simplified by writing an equivalent open loop version as shown in Fig. 4. In Fig. 4:

$$(2) \qquad \frac{\theta(s)}{\bar{F}_0(s)} = \frac{G(s)}{1 + kG(s)} \simeq \frac{8.07(s + 4.56)}{(s + 3.8)(s + 24.2)} \ ,$$

which can be further approximated as

$$(3) \qquad \frac{\theta}{\bar{F}_0}(s) \simeq \frac{k_1}{s + \beta} = \frac{9.7}{s + 24.2}$$

The corresponding differential equation is

$$(4) \qquad \dot{\theta}(t) = -\beta\,\theta(t) + k_1 \bar{F}_0(t) \ .$$

For convenience, we rewrite (4) after scaling as

$$(5) \qquad \dot{\theta}(t) = -\beta\,\theta(t) + G_1(t) + G_2(t)$$

where

$$(6) \qquad G_1(t) = k_1 F_1(t), \ G_2(t) = k_1 F_2(t)$$

are equivalent displacement inputs per unit time.

B. Equation of Motion

Our objective is to study the Langevin type equation (5) and solve for the probability density function (p.d.f.), $\pi(\theta, t \mid \theta_0, 0)$, for target image motion within a local area. This leads us to the evaluation of moments relating to random motion inside a local area which can be checked experimentally, subject to the model limitations.

In equation (5) we are treating a one-dimensional model in which the continuous random variable $\theta(t)$ is subjected to the following types of variations:

a) The change due to the drag term $-\beta\theta$, where β is akin to a friction coefficient.

b) The microsaccadic impulses which occur as independent random events in time contribute to changes in θ by amounts y governed by a known p.d.f. $\varphi(y)$.

c) The high frequency tremor contributes a white noise component to the fluctuations in θ.

The random motions of θ in time t are similar to that of a Brownian particle whose changes of position are that due to a white noise convoluted with contributions arising from a point process.

In equation (6) G_1 possesses the following properties:

$$\langle G_1 \rangle = 0 \tag{7}$$

$$\langle G_1(t)G_1(t')\rangle = D\delta(t-t') \quad ,$$

where D is the covariance of G_1. The microsaccades are modeled herein to occur with a p.d.f. of poisson intensity λ. They cause a jump from θ to $\theta+y$ where the random variable y is governed by a p.d.f. $\varphi(y)$ at all times.

The next section deals with the method of solving for the conditional p.d.f. $\pi(\theta, t|\theta_0, 0)$.

III. The Equation for $\pi(\theta, t|\theta_0, 0)$

It is customary to write fokker planck equations for p.d.f. $\pi(\theta, t|\theta_0, 0)$ corresponding to the equation (5) in the absence of the point process represented by $G_2(t)$. In the present case, however, we can still write the partial differential equation for $\pi(\theta, t|\theta_0, 0)$ by standard probability arguments. Since the G_1 process is of high frequency we can write for the changes in θ in a time (Δt) caused by G_1 alone as

$$M(\Delta) = \int_t^{t+\Delta} G_1 \, dt \tag{8}$$

and it is easy to see that in view of equation (7)

$$\mathcal{E}[M(\Delta)] = 0$$

(9) and

$$\lim_{\Delta \to 0} \frac{1}{\Delta} \mathcal{E}[M^2(\Delta)] = D \quad .$$

Arguing out the changes that can take place in a time Δ, we have[2] for $\pi(\theta, t)$

$$\pi(\theta, t) = (1-\lambda\Delta)\pi(\theta + \beta\theta\Delta - M(\Delta), t-\Delta) \tag{10}$$

$$+ \lambda\Delta \int_{-\infty}^{\infty} \pi(\theta-\theta', t)\varphi(\theta')d\theta' \quad .$$

Using Taylor series expansion for the right-hand side of (10) and taking the limit when $\Delta \to 0$, we have

$$\frac{\partial\pi(\theta,t)}{\partial t} = \beta\theta \frac{\partial\pi(\theta,t)}{\partial\theta} + \beta\pi(\theta,t) + \frac{D}{2} \frac{\partial^2\pi(\theta,t)}{\partial\theta^2} - \lambda\pi(\theta,t) \tag{11}$$

$$+ \lambda \int_{-\infty}^{\infty} \pi(\theta-\theta', t)\varphi(\theta')d\theta';$$

$$-\infty < \theta < \infty \quad ,$$

---

[2] We will hereafter write $\pi(\theta, t|\theta_0, 0)$ as $\pi(\theta, t)$ for convenience.

with the boundary conditions represented by

$$\pi(\theta,0) = \delta(\theta-\theta_0)$$

(12)

$$\pi(-\infty,t) = \pi(\infty,t) = 0 \quad .$$

We can apply the transform technique to solve equation (11). Defining the fourier transform for $\pi(\theta,t)$ with respect to θ as

$$\overline{\pi}(w,t) = \int_{-\infty}^{\infty} \pi(\theta,t) e^{iw\theta}\, d\theta \quad . \tag{13}$$

We arrive at the following, assuming $\theta_0 = 0$:

$$\frac{\partial\overline{\pi}(w,t)}{\partial t} + \beta w \frac{\partial\overline{\pi}(w,t)}{\partial w} = \left[\frac{-Dw^2}{2} - \lambda(1-\overline{\varphi}(w)\right]\overline{\pi}(w,t) \quad , \tag{14}$$

where $\overline{\varphi}(w)$ is the fourier transform of $\varphi(y)$. The initial conditions are

$$\overline{\pi}(w,0) = 1; \qquad \overline{\pi}(0,t) = 1 \quad . \tag{15}$$

The partial differential equation (14) can be solved by the method of characteristics and this leads to the following:

$$\overline{\pi}(w,t) = \exp\left\{-\frac{Dw^2}{4\beta}(1-e^{-2\beta t}) + \frac{\lambda}{\beta}\left[F(we^{-\beta t})-F(w)\right]\right\} \quad , \tag{16}$$

where

$$F(w) = \int_0^w \frac{1-\overline{\varphi}(w')}{w'}\, dw' \quad . \tag{17}$$

The inverse fourier transform of (16) will yield $\pi(\theta,t)$ which we are seeking. However, this is difficult to obtain by analytic methods for

$\varphi(y)$ represented by either a gaussian or a bimodal p.d.f. which are of practical interest. We can of course obtain the inverse by numerical methods. Since $\bar{\pi}(w,t)$ is the characteristic function of the stochastic process $\theta(t)$ we can easily evaluate the moments of $\theta(t)$ corresponding to the motion in each local area. Equation (16) makes it clear that if $\lambda = 0$, we have the characteristic function corresponding to the usual Uhlenbeck-Ornstein process [18]. A further analysis of this characteristic function leads us to relate in a simple manner the cumulants of the process $\theta(t)$ to the moments of the p.d.f. $\varphi(y)$ suitably scaled by λ/β. This relationship can be stated as a theorem.

Theorem. If the process $\theta(t)$ is governed by a Langevin type of equation as described by (5), the cumulants K_n of $\theta(t)$ are given by

$$K_n = U_n + \frac{\lambda}{\beta}\frac{m_n}{n}(1-e^{-n\beta t}) \qquad n = 1,2,\ldots \tag{18}$$

where the U_n are the cumulants of the Uhlenbeck-Ornstein process $\theta(t)$ obtained in the absence of the poisson input process represented by G_2 in (5) and the m_n are the moments of the p.d.f. $\varphi(y)$ governing the contributions from the poisson process. Of course, it is well known that

$$U_2 = \frac{D}{2\beta}(1-e^{-2\beta t}) \qquad \text{for } n = 2$$

and

$$U_n = 0 \qquad n \neq 2 \; . \tag{19}$$

To prove the above statement we rewrite the expression $\frac{\lambda}{\beta}[F(we^{-\beta t})-F(w)]$ appearing in (16) in terms of the moments of $\varphi(y)$. In view of (17) we have

$$(20) \qquad \frac{\lambda}{\beta}[F(we^{-\beta t})-F(w)] = \frac{\lambda}{\beta} \sum_{r=1}^{\infty} \frac{i^r}{r!} \frac{s^r}{r} m_r(1-e^{-r\beta t}) \quad .$$

If we designate $\ell n\, \overline{\pi}(w,t)$ as $M(w,t)$ we know that the cumulants are given by

$$(21) \qquad \frac{1}{i^n} \frac{\partial^n M}{\partial w^n} \Bigg|_{w=0} = K_n \quad .$$

Hence

$$(22) \qquad K_n = \frac{D}{2\beta}(1-e^{-2\beta t})\delta_{n,2} + \frac{\lambda}{\beta} \frac{m_n}{n}(1-e^{-n\beta t})$$

where $\delta_{n,2}$ is the kronecker delta. Once the cumulants are obtained it is easy to derive the moments by employing the well-known relations between them.

The experimental data indicate that the occurrence times of microsaccades have a p.d.f. that may be approximated by a poisson process and that $\varphi(y)$ corresponds to a bimodal p.d.f. given by

$$(23) \qquad \varphi(y) = \frac{\alpha^2}{2}|y|e^{-\alpha|y|} \quad .$$

Corresponding to this situation the characteristic function $\overline{\pi}(w,t)$ is:

$$(24) \qquad \overline{\pi}(w,t) = \frac{\mathrm{Exp}-\left\{\left[\frac{Dw^2}{2\beta} + \frac{\lambda}{\beta}\frac{\alpha^2}{2}\frac{w^2}{\alpha^4+w^2(1+e^{-2\beta t})+w^4e^{-2\beta t}}\right](1-e^{-2\beta t})\right\}}{\left(\frac{\alpha^2+w^2}{\alpha^2+w^2e^{-2\beta t}}\right)^{\frac{\lambda}{2\beta}}}$$

and the first two moments of $\theta(t)$ for the local area motion are given by

$$
\begin{aligned}
&< \theta(t) > = 0 \\
&< \theta^2(t) > = \frac{D}{2\beta}(1-e^{-2\beta t}) + \frac{\lambda}{\beta}\frac{m_2}{2}(1-e^{-2\beta t})
\end{aligned}
\tag{25}
$$

with $m_2 = 4/a^2$.

Higher order moments may be computed if necessary. These features regarding the local area motion can be checked with the experimental findings as discussed in Section V.

IV. The Large Saccades and Reference Changes

It will be our aim to bring into the framework of our model the phenomenon of reference changes that occurs in transferring the image point from one local area to another. We say that when the image point has remained too long in a given local area, a large saccade is likely to occur and the probability of the large saccade occurring increases with the time of stay within a local area. Let us set limits of a given local area, as

$$-a \leq \theta \leq +a \quad .$$

The idea of an increased probability of the large saccade as a function of time spent in a local area has a physiological basis. Presumably neural adaptation increases as a function of the time spent in a local area thereby increasing the utility of switching to a new local area.

When the large saccade occurs and the image point is transferred to another local area, we assume that to all intents, the image point starts moving from the foveal axis, i.e., from the initial point $\theta_0 = 0$ again. The whole process therefore is repeated again till the next large saccade occurs. So we can safely say that at $t = 0$, a large saccade has occurred and the θ_0 is set to zero from this time onwards. Let us say that the probability for the next large saccade

to occur is given by $p(a,t)$ at any time, t, given that one has occurred at $t = 0$, where we assume that $p(a,t)$ is given as:

$$p(a,t) = 1 - \int_{-a}^{a} \pi(\theta,t)d\theta. \tag{26}$$

Note that $p(a,t)$ will increase with time thereby increasing the likelihood of a large saccade as desired. This is a very simplified assumption and reveals that the occurrence of large saccades form a renewal process, with $p(a,t)$ as the renewal density. Once we have this renewal function, the product density $h(t)$, introduced by Ramakrishna [19], of the large saccade occurring at any time, t, is given by

$$h(t) = p(a,t) + \int_{0}^{t} p(a,\tau)h(t-\tau)d\tau \tag{27}$$

Taking Laplace transforms on both sides, we have for $\tilde{h}(s)$, where

$$\tilde{h}(s) = \int_{0}^{\infty} h(t)e^{-st}\,dt \quad , \tag{28}$$

the expression

$$\tilde{h}(s) = \frac{\tilde{p}(s)}{1 - \tilde{p}(s)} \quad . \tag{29}$$

Thus we have the product density for the occurrence of the large saccade from which it is easy to calculate the mean and moments of the number of large saccades that occur within a time 0 to T. The mean of the number of times that changes of local areas occur in T seconds is given by

$$(30) \qquad \langle N(T) \rangle = \int_0^T h(t)dt$$

and mean square by

$$(31) \qquad \langle N^2(T) \rangle = \int_0^T h(t)dt + \int_0^T \int_0^T h(t_1)h(t_2-t_1)dt_1dt_2 \quad .$$

These quantities can be experimentally checked and the validity of the stochastic model described above may be estimated.

V. Experimental Data and Results

In order to validate the model predictions made in Section III, we must first know the statistics of the two driving inputs $G_1(t)$ the tremor, and $G_2(t)$, the point process representing the microsaccades. This means that we must find the values of D ($min^2/sec.$), the covariance of G_1, λ (1/sec.) the poisson intensity of microsaccade occurrences and an expression for $\varphi(y)$, the p.d.f. of the microsaccade amplitudes. Unfortunately, for humans, we have no way of acquiring this information directly from measurements on $G_1(t)$ and $G_2(t)$. Hence, our only recourse is to use the only available data, namely, the time records of eye movements during fixation.

A typical example of eye movement data during fixation is shown in Fig. 5. This data was acquired by means of a reflection technique utilizing infrared light and a bridge circuit with photodiodes [20,21].

In the figure, large saccades that separate periods of local area activity are indicated. During the local area activity microsaccadic transients and smooth eye movement (physiological drift) are evident. Most of the tremor component of eye movements are not visible. This is because these tiny oscillations are in the noise level of this recording technique, accurate to ± 15 seconds of arc. The components in the data, $\theta(t)$, corresponding to the tremor and

microsaccade driving inputs are separated by appropriate digital filtering. The data sampling rate was 60 samples per second and the minimum velocity threshold for editing the microsaccades was set at 300 minutes of arc per second. This precluded the measurement (or editing) of microsaccades of amplitudes smaller than 5 minutes of arc. In Fig. 6 an amplitude histogram for the microsaccades is presented. In constructing this histogram we have combined the data for right and left microsaccades; this is satisfactory since we are assuming left-right symmetry in the data. As mentioned earlier the smallest amplitude measured is 5 minutes of arc. However, data from Beeler [22] indicate that the frequency of occurrence of the microsaccades decreases for amplitudes less than 10 minutes of arc, instead of 5 minutes of arc. Also, as might be expected from biological data, this estimate reveals intersubject variation ranging from 5 to 10 minutes of arc. The histogram in Fig. 6 leads us to choose a bimodal p.d.f. as in (23) for $\varphi(y)$, the microsaccade amplitude p.d.f., with the value of 0.1 (minutes^{-1}) assigned to α.

To evaluate λ, the poisson intensity of the microsaccade occurrences, we need the intersaccadic interval histogram from data as presented in Fig. 7. The interval histogram of Fig. 7 is not as expected for a poisson process.

It indicates that the occurrences of microsaccades are not independent as assumed earlier but in fact are correlated. A similar situation is seen with the effect of the absolute refractory period in neural spike train interval histograms. Modifications of the theory due to this fact will be presented in a future report. For the purpose of this paper we assume a poisson process as a good approximation to represent the microsaccade occurrences, and find that λ is 3 (sec.$^{-1}$).

The work of Beeler [22] provides measurements of tremor amplitude as a function of frequency. From this data we can very easily obtain the value for $[\overline{\theta^2(t)}]_{tremor}$. This quantity can now be related to D, the covariance of G_1 by the expression:

$$(32) \qquad [\overline{\theta^2}(t)]_{tremor} = \frac{D}{2\pi j}\int_{-j\infty}^{j\infty}\left(\frac{1}{s+\beta}\right)\left(\frac{1}{-s+\beta}\right)ds$$

$$= \frac{D}{2\beta}$$

where β is the inverse time constant of the equivalent open-loop plant of Fig. 4. Solving (32) for D gives it a value of 0.05265 minutes^2/second.

Now we have all the parameter values needed to evaluate the first two moments of $\theta(t)$ as given by (25). The upper bounds for values of these moments are given by the expressions

$$(33) \qquad \begin{aligned} &< \theta(t) >_u = 0 \\ &< \theta^2(t) >_u = \frac{D}{2\beta} + \frac{\lambda}{\beta}\frac{m_2}{2} \end{aligned}$$

where $m_2 = \frac{4}{\alpha^2}$ for $\varphi(y)$ as in (23). Substituting for D, β, λ and α in (33) we get:

$$(34) \qquad \begin{aligned} &< \theta(t) >_u = 0 \\ &< \theta^2(t) >_u \simeq 24 \text{ (minute)}^2 \end{aligned}$$

or a root mean square value of the movement of approximately 5 minutes. Preliminary estimates from our data give root mean square values for $\theta(t)$ between 3 to 11 minutes with an average of 7 minutes. This is within the expected range of the predicted value of 5 minutes.

VI. Conclusions

We have considered here a very simplified model of the eye movements during fixation on a target. The concept of local area movements of the image point and the transference of local areas

from time to time by the occurrence of large saccades are the central features of the model. The random movements inside each local area are caused by the jump processes called microsaccades, the high frequency tremor noise, and the compensatory drift. The p.d.f. $\pi(\theta,t)$ governing these local area wanderings can be obtained from equation (10) of the text. Numerical inversion of the fourier transform $\overline{\pi}(w,t)$ is being carried out. Even without obtaining the inverse transform, we are able to evaluate the moments of the displacements within each local area by the use of the theorem stated in Sec. III, equation (25). From the experimental data presented in Sec. V, the standard deviation for such motions arrived at from this model is of the order of 5 minutes of arc which checks favorably with the actual experimental data. The renewal density of the large saccades is arrived at by a simple criterion. The Laplace transform of the product density of the occurrence of large saccades is obtained in equation (29). Numerical inversion of the transforms and the calculation of the mean and moments of the number of large saccades occurring in a given time are in progress. Sophistications of this model incorporating more realistic criteria for the occurrence of large saccades, and the microsaccades will be reported in a later contribution. Several extensions of this work are planned. The first involves modifications in our analyses to allow for eye movements in two dimensions; the second is an appropriate iteration of our model to describe eye movements during continuous visual tracking tasks; and the third concerns applications of this approach to other related topics.

We are also planning a careful reassessment of the local area hypothesis from measurements of vertical as well as horizontal eye movements. The local area hypothesis involves a specialized part of the retina, the fovea, which is used to process visual images; furthermore at any one time only a portion of the fovea, a local area, receives the target image. The implication of this model is that the fovea has a uniform visual acuity and hence all parts of the fovea have equal likelihood of being chosen as the next local area. This, in fact, is not the case because visual acuity is at a maximum at

the center of the fovea and decays to a tenth of this value at the edge of the fovea. This suggests that the spatial distribution of the local areas within the fovea might well be dependent on such a feature.

It was assumed in Sec. IV that a transition from one local area to another is such that the reference point for the new local area coincides with the position of the image point at the termination of the large saccade. This allowed us to take $\theta_0 = 0$ as the initial condition prior to start of motion within a local area. In reality, however, this hypothesis does not hold strictly and θ_0 must be assumed to be a random variable with some a priori p.d.f. $p(\theta_0)$. A suitable modification to our analysis is thus warranted.

Finally, in extending the model to tracking tasks it will be necessary to replace Robinson's model [15] for the plant by a more appropriate nonlinear model such as the one proposed by Cook and Stark [17]. Applications of the approach taken in this paper seem plausible in allied fields such as neurophysiology and communications theory.

REFERENCES

1. Stark, L., G. Vossius, and L. R. Young, "Predictive Control of Eye Tracking Movements," IRE Trans. Human Factors in Electronics, Vol. 3, 1962, pp. 52-56.

2. Young, L. R., and L. Stark, "Variable Feedback Experiments Testing a Sampled Data Model for Eye Tracking Movements," IEEE Trans. Human Factors in Electronics, Vol. 4, 1963, pp. 38-51.

3. Cook, G., and L. Stark, "Derivation of a Model for the Human Eye Positioning Mechanism," Bull. Math. Biophys., Vol. 29, pp. 153-174.

4. Ditchburn, R. W., and D. H. Fender, "The Stabilized Retinal Image," J. Physiol., Vol. 119, 1953, pp. 1-17.

5. Ditchburn, R. W., and B. L. Ginsborg, "Involuntary Eye Movements During Fixation," Nature, Vol. 170, 1952, p. 36.

6. Nachmias, J., "Determiners of the Drift of the Eye During Monocular Fixation," J. Op. Soc. Am., Vol. 51, No. 7, 1961, pp. 761-766.

7. Nachmias, J., "Two-dimensional Motion of the Retinal Image During Monocular Fixation," J. Op. Soc. Am., Vol. 49, No. 9, 1959, pp. 901-908.

8. Proskuryakova, N. G., and A. R. Shakhnovich, "Quantitative Characteristics of Fixation Micromovements of the Eye," Biofizika, Vol. 13, No. 6, 1967, pp. 117-126.

9. Riggs, L. A., J. C. Armington, and A. Ratliff, "Motions of the Retinal Image During Fixation," J. Op. Soc. Am., Vol. 44, No. 4, 1954, pp. 315-321.

10. Cornsweet, T. N., "Determination of the Stimuli for Involuntary Drifts and Saccadic Eye Movements," J. Op. Soc. Am., Vol. 46, No. 11, 1956, pp. 987-993.

11. Boyce, P. R., "Monocular Fixation in Human Eye Movement," Roy. Soc., (L) Proc. Series B, Vol. 167, 1967, pp. 293-315.

12. Ditchburn, R. W., et al., "Vision with Controlled Movements of the Retinal Image," J. Physiol., Vol. 145, No. 1, 1959, pp. 98-107.

13. Smith, J. D., and A. V. Phatak, "Eye Movements During Fixation on a Stationary Target: Preliminary Data and Synthesis of a Model," San Diego Biomedical Symposium, February, 1971.

14. Westheimer, G., "Mechanism of Saccadic Eye Movements," AMA Arch. Opthalmol., Vol. 52, 1954, pp. 710-724.

15. Robinson, D. A., "The Mechanisms of Human Saccadic Eye Movement," J. Physiol., Vol. 174, 1964, pp. 245-264.

16. Robinson, D. A., "The Mechanisms of Human Smooth Pursuit Eye Movement," J. Physiol., Vol. 180, 1965, pp. 569-591.

17. Cook, G., and L. Stark, "Dynamic Behavior of the Human Eye-positioning Mechanism," Comm. Beh. Biol., Part A, Vol. 1, 1968, pp. 197-204.

18. Uhlenbeck, G. E., and L. S. Ornstein, "On the Theory of the Brownian Motion," Physical Review, Vol. 36, 1930; reprinted in "Selected Papers in Noise and Stochastic Processes," Nelson Wax, Dover Pub., New York.

19. Ramakrishna, A., "Stochastic Processes Relating the Particles Distributed in a Continuous Infinity of States," Proc. Cam. Phil. Soc., Vol. 46, 1950, p. 595.

20. Gauthier, G. M., Bioengineering Studies of Cerebellar Influences on Oculomotor Control, Ph.D. Dissertation, University of Illinois Medical Center, 1970.

21. Young, L. R., "Measuring Eye Movements," Am. J. Med. Electronics, Vol. 2, 1963, pp. 300-307.

22. Beeler, G. W., Stochastic Process in the Human Eye Movement Control System, Ph.D. Dissertation, California Institute of Technology, 1965.

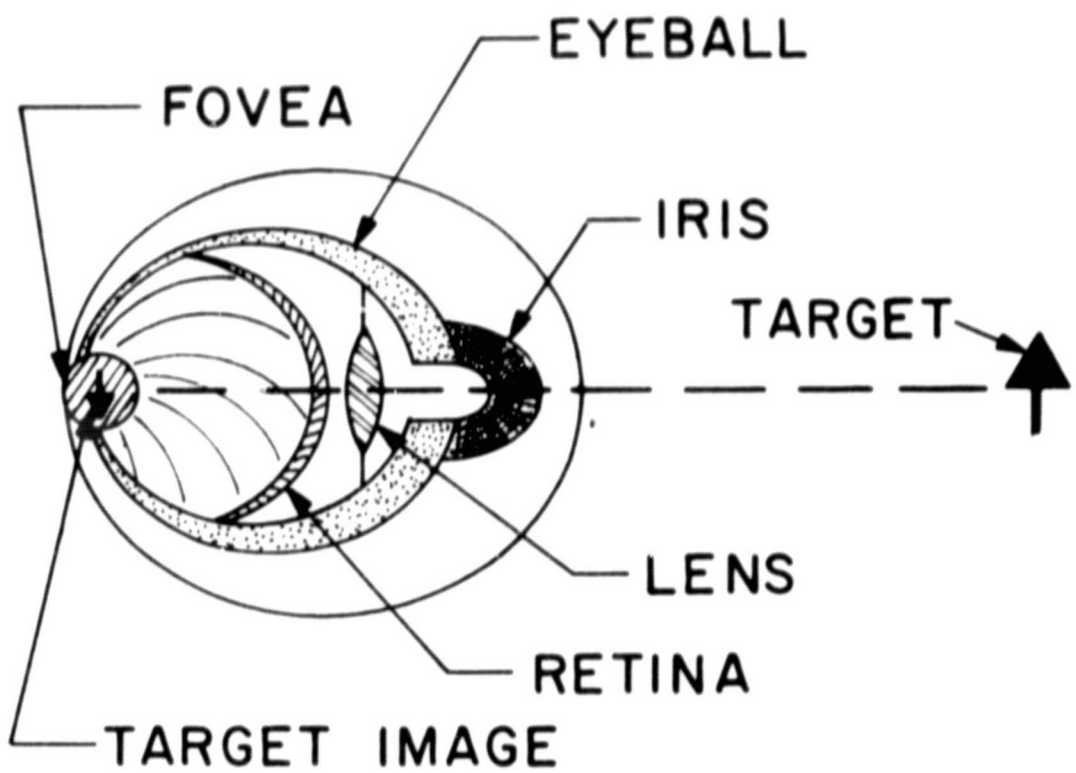

Figure 1

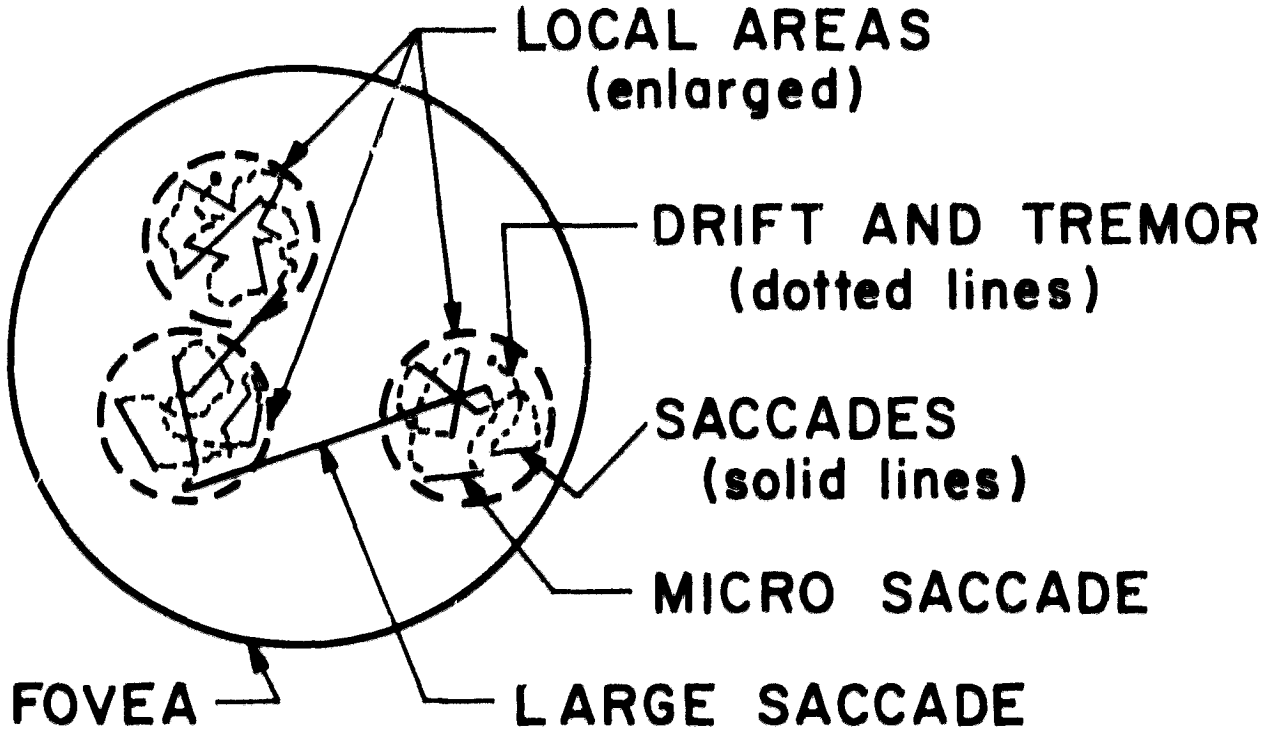
LOCAL AREAS
(enlarged)
DRIFT AND TREMOR
(dotted lines)
SACCADES
(solid lines)
MICRO SACCADE
FOVEA
LARGE SACCADE

Figure 2

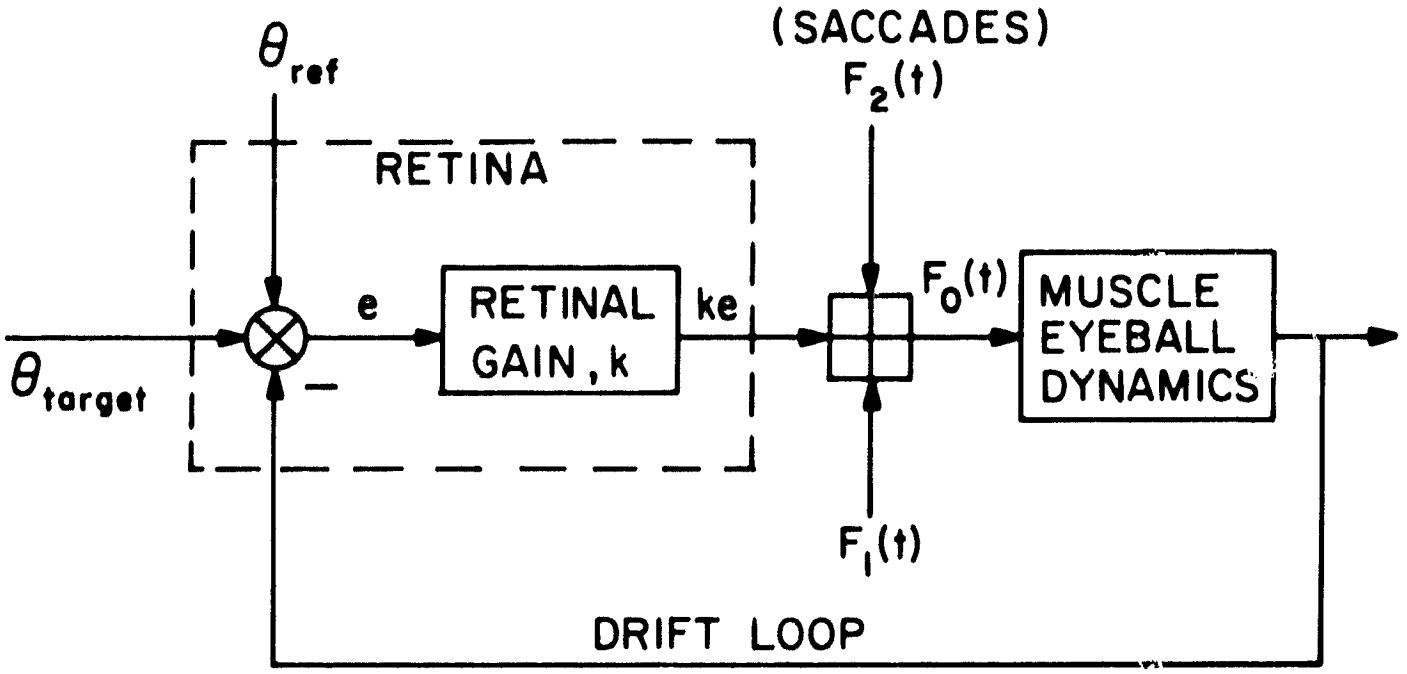
θ_{ref}
(SACCADES)
$F_2(t)$
RETINA
e
RETINAL GAIN, k
ke
$F_0(t)$
MUSCLE EYEBALL DYNAMICS
θ_{target}
−
$F_1(t)$
DRIFT LOOP

Figure 3

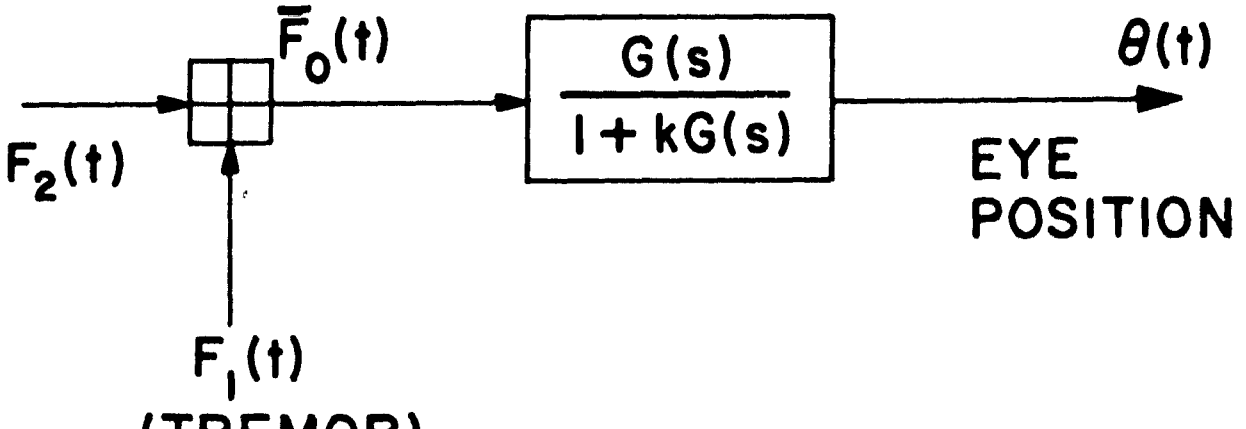

Figure 4

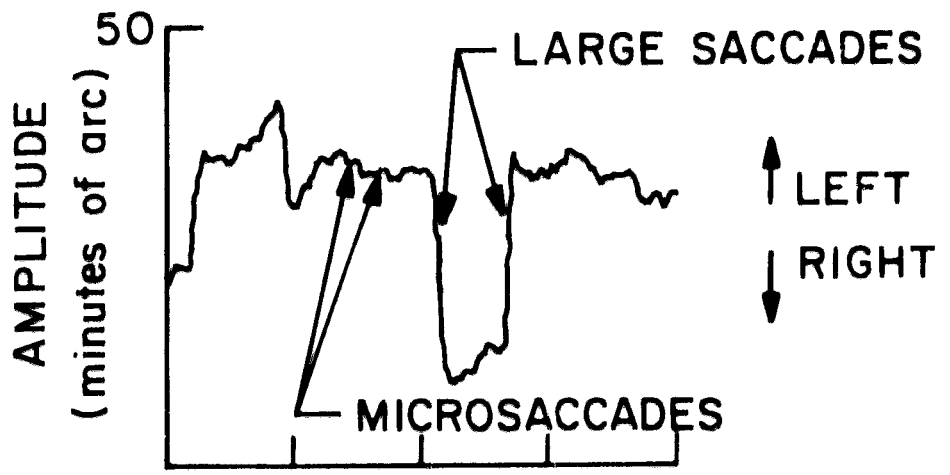
50
AMPLITUDE
(minutes of arc)
LARGE SACCADES
LEFT
RIGHT
MICROSACCADES
0
1
2
3
4
TIME (seconds)

Figure 5

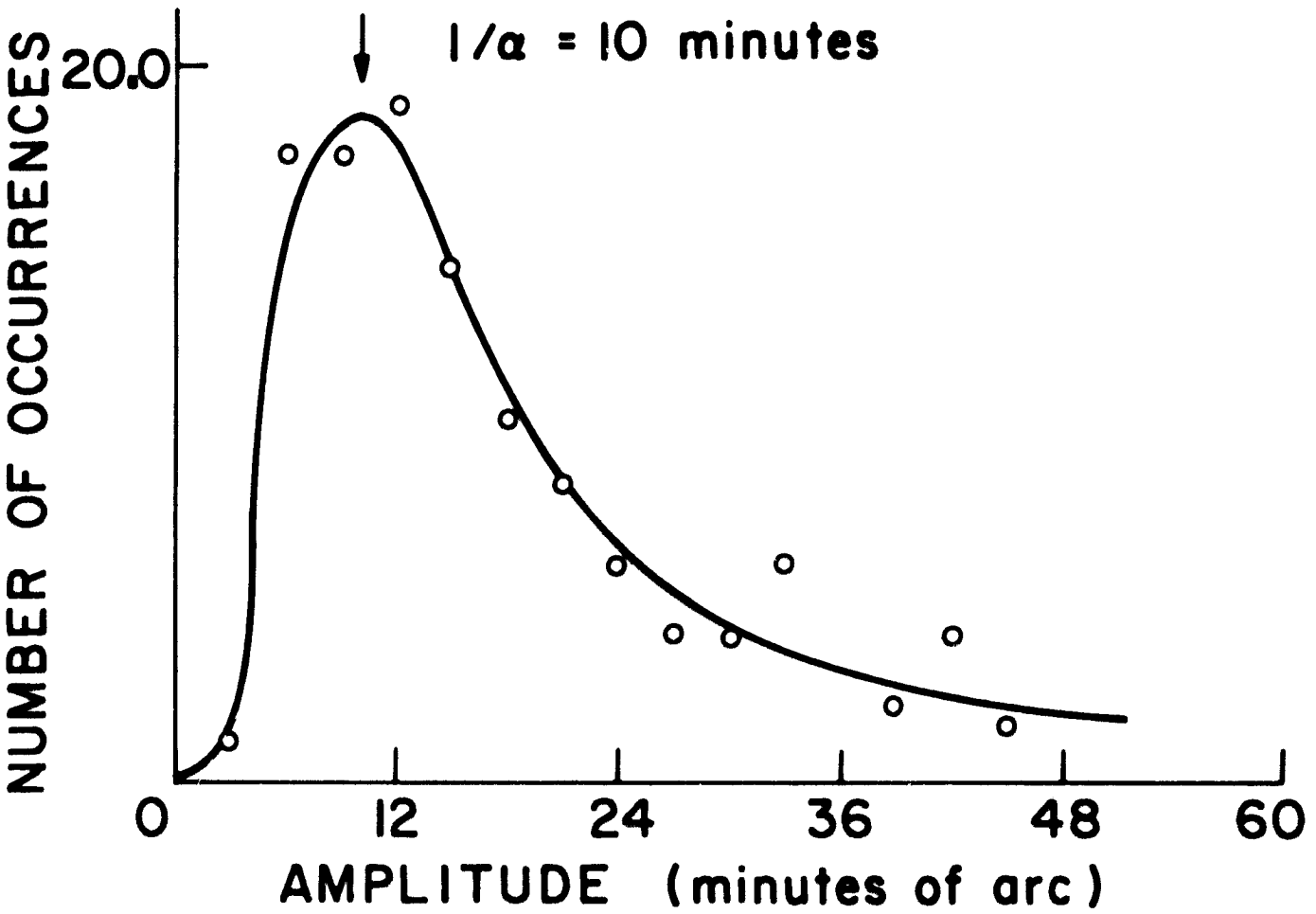
1/α = 10 minutes
20.0
NUMBER OF OCCURRENCES
0
12
24
36
48
60
AMPLITUDE (minutes of arc)

Figure 6

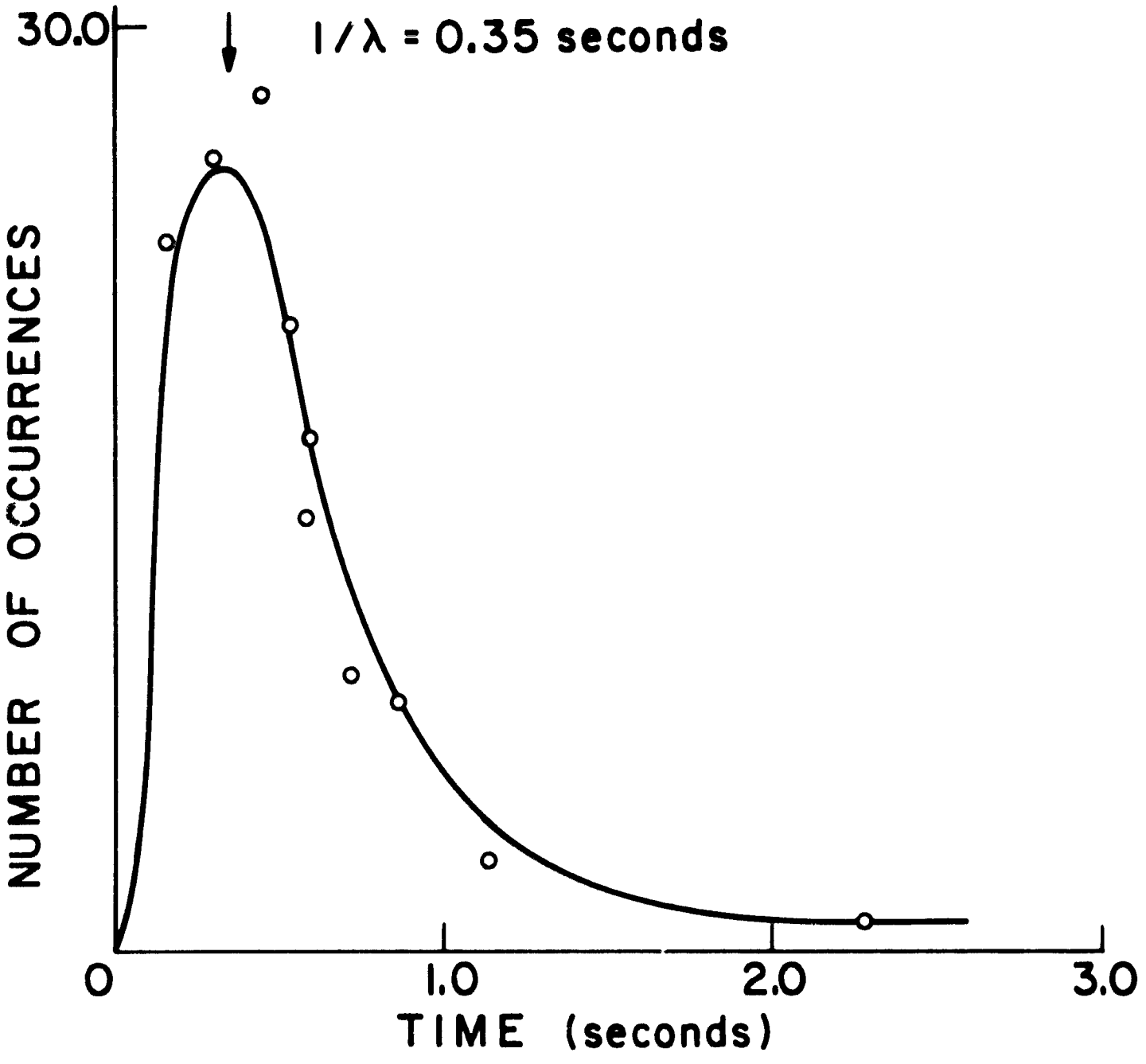
30.0
1/λ = 0.35 seconds
NUMBER OF OCCURRENCES
0
1.0
2.0
3.0
TIME (seconds)

Figure 7